



Cite this: *Polym. Chem.*, 2024, **15**, 3675

A sulfur copolymer with a pyrrole compound for the crosslinking of unsaturated elastomers†

Simone Naddeo, Vincenzina Barbera * and Maurizio Galimberti *

Effective applications must be found for sulfur, a widely available and inexpensive element. Over the last decade, copolymers with unsaturated comonomers have been prepared *via* so-called inverse vulcanization. In this work, a sulfur copolymer with a circular and biosourced di-pyrrole compound was obtained for the first time and was used as the sole crosslinking agent of an unsaturated elastomer. Pyrrole compounds (PyCs) were synthesized *via* the Paal–Knorr reaction of 2,5-hexanedione (HD) and hexamethylenediamine (HMD) or ethylenediamine (EDM). The PyCs were obtained without using solvents or catalysts in high yield and with water as the only co-product. Poly(S-*co*-HMDP) and poly(S-*co*-EDP) copolymers were prepared under the typical conditions of inverse vulcanization. Throughout the entire synthetic pathway, the overall yield was up to 92% and the atom efficiency was up to 73%. The *E*-factor evaluated for organic compounds was almost null. The sulfur weight content in the copolymers ranged from 40% to 80% and the average number of sulfur atoms in the sequences ranged from 3 to 17. The copolymers were found to be amorphous with a glass transition temperature ranging from –2 to 38 °C, increasing with the content of the pyrrole ring. The number average molecular weight was found to be in the range from 1500 to 9000 g mol^{–1}. The molecular weight distribution was pretty narrow, with values lower than 2. NMR investigation suggested that the β position of the pyrrole ring reacted with sulfur atoms. A poly(S-*co*-HMDP) copolymer with an average sequence of 3 sulfur atoms was used as the sole crosslinking agent in a composite based on an unsaturated elastomer such as poly(styrene-*co*-butadiene) from anionic polymerization. More efficient crosslinking was obtained by promoting the ionic reaction of sulfur with elastomer chains by using 1,5-diazabicyclo[5.4.0]undec-7-ene. These results pave the way for the synthesis of a wide variety of sulfur copolymers with comonomers containing pyrrole rings for the sustainable crosslinking of elastomers, avoiding the use of oil-based accelerators.

Received 25th June 2024,
Accepted 11th August 2024

DOI: 10.1039/d4py00706a

rsc.li/polymers

1. Introduction

Sulfur is a widely available and inexpensive building block. It is a common element in the Earth's crust, present at levels of about 620 parts per million, primarily in volcanic areas.¹ It has been mined for centuries and used in various applications, including medicine,^{2,3} as religious incense,⁴ to reduce the stickiness of natural rubber in the fabrication of raincoats,⁵ for bleaching fabrics, as an insecticide and as a colorant.⁶ Sulfur has been used for the vulcanization of elastomers since the nineteenth century.^{7,8} Nowadays, elemental sulfur is primarily

obtained as a by-product of the oil and gas industry. Concerns about acid rain caused by sulfur oxides and catalyst deactivation in refining processes have been the driving forces in the hydrodesulfurization of crude oil. As a result, a huge amount of sulfur is available, around 70 million tons worldwide every year.⁹ Sulfur is not toxic, but is flammable, which necessitates the removal of accumulated sulfur stockpiles. Sulfur is prevailingly used for the preparation of chemicals, mainly sulfuric acid,¹⁰ but there is great potential for the synthesis of innovative materials starting from waste.

Sulfur can exist in several allotropic forms. S₈ rings are packed in an orthorhombic cell up to 96 °C and in a monoclinic cell up to 119 °C. Sulfur begins to melt at 120 °C and forms rings of 8–35 atoms. At 159 °C (the floor temperature), equilibrium ring-opening polymerization occurs, producing linear polysulfanes with radical chain ends, which polymerize into high molecular weight polymeric sulfur. In a seminal work,¹¹ diradicals were quenched with 1,3-diisopropenylbenzene (DIB), performing radical copolymerization of sulfur and DIB at 185 °C, in molten liquid sulfur, with a method known

Politecnico di Milano, Department of Chemistry, Materials and Chemical Engineering “G. Natta”, Via Mancinelli 7, 20131 Milano, Italy.

E-mail: vincenzina.barbera@polimi.it, maurizio.galimberti@polimi.it, simone.naddeo@polimi.it

† Electronic supplementary information (ESI) available: ¹H and ¹³C NMR spectra, GC-mass and ESI-mass analysis of the monomers, GPC analysis and Hansen solubility parameters of poly(S-*co*-PyC). See DOI: <https://doi.org/10.1039/d4py00706a>



as inverse vulcanization. A thermoplastic processable copolymer was obtained, usable in Li-S batteries. Inverse vulcanization has also been used to prepare other sulfur copolymers with various comonomers, including the following: 1,3-diethylbenzene,¹² divinylbenzene,¹³ limonene,¹⁴ styrene,¹⁵ poly(4-allyloxystyrene) (PAOS),¹⁶ diallyl sulfide,¹⁷ poly(allyl-benzoxazine),¹⁸ dicyclopentadiene, farnesene and myrcene,¹⁹ cardanol,²⁰ 5-ethylidene-2-norbornene,²¹ canoa oil,²² aliphatic diamines and diisocyanides to obtain polythioureas,²³ a mixture of α , β -pinene, limonene and 3-carene,²⁴ pentaerythritol tetra(3-mercaptopropionate),²⁵ and 4-vinylbenzyl chloride.²⁶ Amorphous copolymers were obtained (minor crystallinity was shown by the copolymer with diallyldisulfide¹⁷), with glass transition temperatures ranging from -13 °C to 115 °C. These sulfur-based copolymers can be used in a variety of applications, such as sulfur-lithium batteries,^{11–13,15,20,21} for the removal of heavy metals from water solutions,^{14,18,19,22–24} as durable and recyclable materials for petrochemical applications,¹⁶ as thermal insulators and infrared optic materials,¹⁷ and as three-dimensional shape memory devices for biological and mechanical applications.^{25,26} The reactivity of carbon allotropes with sulfur and sulfur-based chemicals in the cross-linking system has also been reported.²⁷

Pyrrole compounds (PyCs)²⁸ are experiencing renewed interest, as they are abundant in natural products,²⁹ are used in pharmaceuticals due to their anticancer, antiviral and antifungal properties^{30,31} and can be used for the preparation of novel materials.³²

A pyrrole ring is classified as a “ π -electron excessive” aromatic system, as six π -electrons are delocalized over five annular atoms. The ring is thus susceptible to electrophilic attacks.^{28,33,34} Pyrrole rings also give rise to radical reactions. They were studied favoring a thermal cleavage^{35–37} of C–H bonds and the positions of hydrogen abstraction were studied through reactions with alkyl radicals³⁸ and by using a peroxide.³⁹ The alpha positions were found to be the most reactive. Also the reaction of aryl radicals was observed to occur in alpha positions.⁴⁰ Thio-functionalized pyrroles are documented (in the scientific literature),⁴¹ but the reaction of sulfur and thiyl radicals⁴² with pyrrole compounds has only recently been reported by some of the authors.⁴³ The reaction of dodecanthiol (DSH) with an alpha-substituted pyrrole, namely 1,2,5-trimethylpyrrole (TMP), resulted in the mono-addition of DSH to a beta position of the pyrrole ring, whereas the reaction of either 1,2,5-trimethylpyrrole or 1-hexyl-2,5-dimethyl-1H-pyrrole with sulfur led to S₃ and S₅ rings between the alpha

methyl and the beta position of the pyrrole ring. The reaction of the pyrrole compound with sulfurated reagents was found to be highly efficient. Indeed, a pyrrole compound, namely 2-(2,5-dimethyl-1H-pyrrol-1-yl)-1,3-propanediol (SP) (chemical structure shown in Fig. 1), was used as a coupling agent between silica and an unsaturated elastomer in a composite suitable for tyre compounds, achieving dynamic-mechanical reinforcement similar to that obtained with traditional coupling agents, such as sulfur based silanes.⁴³ The Si(OH) groups reacted with silica and the pyrrole ring with sulfur and sulfur based chemicals, despite its lower concentration with respect to the unsaturated elastomer; there was one pyrrole ring for every fifty double bonds and for every four vinyl groups.

The radical reactivity of pyrroles results from the easy homolytic extraction of hydrogen, which leads to an sp² carbon radical, stabilized *via* the neighbouring π electrons. Two hybrids are formed, which can facilitate the substitution of the pyrrole ring either in the alpha or in the beta position. The termination occurs *via* coupling with a radical species, a thiyl radical in the reported example.⁴³

In light of these results, the pyrrole ring appears to be suitable for quenching polysulfane diradicals under typical inverse vulcanization conditions, similar to the conditions used in the first work.¹¹ for this type of polymerization. Innovative polymers can be formed. Indeed, the pyrrole ring is the first example of a reactive group other than double bonds for the synthesis of sulfur copolymers. Using pyrrole as the reactive group opens the possibility of incorporating a wide variety of comonomers, which can be prepared from diamines as well as from unsaturated amines and which can give rise to a multitude of copolymers with adjustable properties. Moreover, the pyrrole ring offers the possibility of using an end-of-life (EOL) material and a bio-sourced reagent for the preparation of the comonomer.

Indeed, in this work, 1,6-diaminohexane was used for preparing 1,6-bis(2,5-dimethyl-1H-pyrrol-1-yl)hexane (hexamethylenediaminopyrrole, HMDP), whose chemical structure is shown in Fig. 1. 1,6-Diaminohexane could be prepared through the hydrolysis of EOL polyamide(6,6).⁴⁴ HMDP was synthesized *via* the Paal-Knorr reaction^{45,46} between 1,6-diaminohexane and 2,5-hexanedione, which could be obtained from the ring opening of a biosourced molecule, namely 2,5-dimethylfuran, as recently reported by the authors.⁴⁷ The pyrrole rings in the backbone chain are functional groups able to establish strong supramolecular interactions. Segmented copolymers could be prepared, with a rigid pyrrole-based region

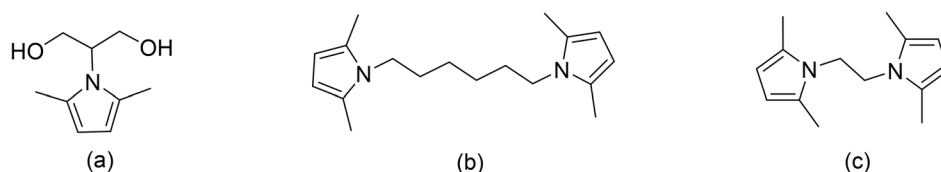


Fig. 1 Chemical structure of (a) 2-(2,5-dimethyl-1H-pyrrol-1-yl)-1,3-propanediol (SP), (b) 1,6-bis(2,5-dimethyl-1H-pyrrol-1-yl)hexane (HMDP) and (c) 1,2-bis(2,5-dimethyl-1H-pyrrol-1-yl)ethane (EDP).



alternating with other sequences, made from sulfur atoms and methylene groups. A higher concentration of the pyrrole rings could enhance the glass transition of the copolymers. To verify this, copolymers of sulfur were also prepared with 1,2-bis(2,5-dimethyl-1H-pyrrol-1-yl)ethane (EDP), whose chemical structure is shown in Fig. 1. The characterization of di-pyrrole compounds was carried out by means of gas chromatography-mass spectrometry (GC-MS), electrospray ionization mass spectrometry (ESI-MS), ¹H-NMR and ¹³C-NMR, and differential scanning calorimetry (DSC). Copolymers were prepared by reproducing prototypical experimental conditions,¹¹ with the sulfur content ranging from 41% to 80% by weight. The sulfur content involved in the synthesis of poly(*S*-co-EDP) was 54%. The chemical composition of the copolymers was assessed through elemental analysis and solubility tests allowed us to determine the solubility parameters. The functional groups of the poly(*S*-co-HMDP) and poly(*S*-co-EDP) copolymers were analyzed by means of Fourier transform infrared (FT-IR) spectroscopy. The molecular weight and molecular weight distribution were assessed using gel permeation chromatography (GPC), and the melting point (m.p.) and glass transition temperature (T_g) of monomers and copolymers were determined through differential scanning calorimetry (DSC). The microstructure of the copolymers and, in particular, the positions of the pyrrole ring reactive with sulfur were investigated by means of ¹H-, ¹³C-, 2D ¹H-¹H-COSY and 2D ¹H-¹³C HSQC NMR.

Entropic elasticity is an indispensable property that allows elastomers to be used in highly demanding applications too, such as in tyre compounds. To achieve entropic elasticity, elastomer chains must be crosslinked through chemical bonds. Crosslinking of elastomers dates back to ancient mesoamericans.⁴⁸ Vulcanization, *i.e.* the crosslinking based on sulfur, was discovered by Charles Goodyear in the XIX century.⁷ Sulfur based crosslinking is widespread and is due to the use of a multicomponent system, which is based on sulfur and one or more accelerators, usually sulphenamides, thiazoles, thiuramides and carbamates.⁴⁹ Secondary accelerators, typically primary amines, are also used.⁴⁹ The accelerators are oil based compounds, also characterized by critical safety data sheets.⁵⁰ The use of a simpler vulcanization system based on a circular biosourced molecule would therefore be desirable. The objective of this work was to use a poly(*S*-co-HMDP) copolymer as the only crosslinking agent. An elastomer composite suitable for tyre compounds was used based on poly(styrene-*co*-butadiene) from solution anionic polymerization (SBR). The crosslinking reaction and the dynamic mechanical properties were investigated by applying sinusoidal stress in shear mode.

2. Experimental section

2.1. Materials

2.1.1. For the synthesis of PyCs (HMDP and EDP). 2,5-Hexanedione, hexamethylenediamine and ethylenediamine were purchased from Sigma Aldrich.

2.1.2. For the synthesis of poly(*S*-co-PyC)copolymers. HMDP and EDP were used as the pyrrole compounds. Sulfur was from ZOLFININDUSTRIA S.r.l.

2.1.3. For the preparation of rubber compounds. SBR (HP755B) was from JSR and had the following chemical composition (wt%): styrene 39.5, vinyl groups 38.2, and extension oil (TDAE, Treated Distillate Aromatic Extract) 37.5. CB N234 was from Cabot Corporation. Stearic acid was from OLEO s.r.l. *N*-(1,3-Dimethylbutyl)-*N*'-phenyl-*p*-phenylenediamine (6PPD) was from Eastman. Zinc oxide was from Lanxess and was supported on a 20% polymeric ligand as the dispersing agent. Oil (Vivatec) was from Hansen and Rosenthal. Sulfur was the same as that used for the preparation of the copolymers.

2.2. Preparation of di-pyrrole compounds (PyC)

2.2.1. Synthesis of 1,6-bis(2,5-dimethyl-1H-pyrrol-1-yl)hexane (HMDP). The synthesis proceeded through the reaction between a primary amine and 2,5-hexanedione, which could be prepared from 2,5-dimethylfuran.⁴⁷ In the following procedure, a commercial sample of HD was used.

In a two-neck round bottom flask, hexamethylenediamine (36.6 mmol, 4.27 g) and water (10 mL) were added in sequence. The mixture was stirred at 37 °C for 30 minutes until a homogeneous solution was obtained. Then, 2,5-hexanedione (73.25 mmol, 8.62 mL) was added dropwise to the solution at 37 °C. The temperature was increased to 120 °C and the reaction mixture was stirred for three hours and was then washed with water in order to remove impurity traces. HMDP was isolated by filtration on filter paper and was dried at 1 atm pressure. A pale-white solid was obtained: 9.0 g, 92% yield, and atom efficiency = 73%. By neglecting the water used for washing HMDP, thus considering only the organic compounds, the *E*-factor⁵¹ was estimated to be 0.46.

¹H-NMR (CDCl₃), δ (ppm): 5.75 (s, 4H), 3.73–3.70 (m, 4H), 2.21 (s, 12H), 1.67–1.59 (m, 4H), 1.43–1.34 (m, 4H).

¹³C-NMR (CDCl₃), δ (ppm): 127.28, 105.12, 43.60, 31.06, 26.84, 12.57.

GC-mass: retention time = 24.20 minutes; molecular peak = 272 m/z.

ESI-mass: [M + H]⁺: calculated exact mass = 273.22 m/z; found exact mass = 273.3 m/z.

2.2.2. Synthesis of 1,2-bis(2,5-dimethyl-1H-pyrrol-1-yl)ethane (EDP). In a two neck round bottom flask, 2,5-hexanedione (42.5 mmol, 4.85 g, 5.0 mL) was added. Then, the flask was placed in an ice-bath for 10 minutes. Ethylenediamine (21.25 mmol, 1.28 g, 1.42 mL) was then added dropwise at 0 °C. A pale white solid was obtained after a few minutes. The reaction mixture was allowed to reach room temperature and was stirred for two hours. Finally, the final reaction crude was washed with water in order to remove impurity traces. EDP was isolated by filtration on filter paper and dried at room temperature and 1 atm pressure. A pale-white solid was obtained: 4.32 g, 88% yield and atom efficiency = 65%. By neglecting the water used for washing HMDP, thus considering only the organic compounds, the *E*-factor⁵¹ was estimated to be 0.42.



¹H-NMR (CDCl₃), δ (ppm): 5.75 (s, 4H), 3.94 (s, 4H), 2.02 (s, 12H).

¹³C-NMR (CDCl₃), δ (ppm): 127.69, 105.83, 43.99, 11.97.

GC-mass: retention time = 19.84 minutes; molecular peak = 216 m/z.

ESI-mass: [M + H]⁺: calculated exact mass = 216.33 m/z; found exact mass = 217.2 m/z.

2.3. Preparation of poly(S-*co*-PyC) copolymers based on sulfur and either HMDP or EDP

The amounts of sulfur and pyrrole compound (either HMDP or EDP) used for the preparation of the copolymers are shown in Table 1. The experimental procedure is reported as follows.

In a round bottom flask sulfur was introduced and heated at 185 °C for ten minutes until a viscous red liquid was obtained. Then, HMDP or EDP was introduced at 185 °C. The so-obtained reaction mixture was stirred at 185 °C for ten minutes. At the end of the reaction, the crude was cooled down to room temperature. A dark brown solid was obtained for all the chemical compositions of the copolymers.

2.4. Preparation of elastomer composites

The recipes of the rubber compounds are provided in Table 2. The amount of ingredients is expressed in parts per hundred rubber (phr).

Table 1 Synthesis of poly(S-*co*-PyC) copolymers

Entry	Sulfur (g)	PyC (g)	Pyrrole ring		Average length of sulfur sequences ^a
			Mol%	Weight%	
<i>PyC: HMDP</i>					
1 ^b	1.40	2.00	14.34	40.59	3
2	1.50	1.50	12.13	34.58	4
3 ^c	2.10	2.00	11.82	33.71	4
4	1.80	1.20	9.64	27.64	6
5	3.50	1.50	7.19	20.73	9
6	4.0	1.00	4.76	13.82	17
7 ^d	4.50	0.50	2.37	6.91	38
<i>PyC: EDP</i>					
8	2.37	1.98	16.56	39.62	4

^a Number of sulfur atoms. ^b Theoretical weight% of each element: C = 46.6%; H = 5.9%; and N = 6.5%. ^c Theoretical weight% of each element: C = 37.9%; H = 4.8%; and N = 5.3%. ^d Poly(S-*co*-HMDP) was not obtained.

Table 2 Recipes of elastomer composites^a

Elastomer composite	1	2
SBR	100	100
CB N234	45	45
Poly(S- <i>co</i> -HMDP) (entry 1)	1.36	1.36
HMDP	0.80	0.80
S	0.56	0.56
DBU	0	0.26

^a Further ingredients: stearic acid 2 phr, ZnO 2 phr, 6PPD 2 phr, and oil 14 phr.

The same amount of sulfur copolymer was used in both elastomer composites, without using other vulcanizing agents. 1,8-Diazabicyclo[5.4.0]undec-7-ene (DBU) was used as the nucleophilic agent in order to improve the crosslinking efficiency. The composites were prepared in two steps: (i) preparation of the masterbatch and (ii) productive mixing, with the addition of vulcanization agents.

2.4.1. Preparation of the masterbatch. The masterbatch was prepared in two phases in a Banbury type tangential internal mixer having a volume of 1200 cm³.

Phase 1. SBR, 767.4 g, was masticated at 40 °C for 30 seconds at 75 rpm. Then, 191.85 g of CB N234 were added and the compound was mixed for 50 seconds at 40 °C and 75 rpm. Then, stearic acid, 15.35 g, CB N234, 115.11 g, and oil, 107.44 g, were added and the compound was mixed for 1 minute and 15 seconds at 40 °C and 75 rpm. The compound was then discharged.

Phase 2. The compound was remixed at 40 °C for 30 seconds at 75 rpm and then, CB N234, 36.95 g, zinc oxide, 14.78 g, and 6PPD, 14.78 g, were added. The obtained compound was mixed for 1 minute and 15 seconds at 40 °C and 75 rpm. Finally, the compound was discharged at 155 °C for 55 seconds at 75 rpm. 1.263 kg of masterbatch were obtained.

The same masterbatch was used for both composites.

2.4.2. Productive mixing: addition of vulcanization agents. The procedure consisted of two phases: (i) masterbatch mastication for 1 minute at 80 °C and 50 rpm and (ii) addition of the crosslinking agents and, optionally, of DBU as the nucleophilic catalyst and then mixing for 2 minutes at 80 °C and 50 rpm.

2.5. Characterization methods

2.5.1. Characterization of the PyCs: HMDP and EDP

GC-MS. The instrument for GC-MS analysis was an Agilent 5973 network mass selective detector with a 6890 series GC system mass spectrometer. The column used for all analyses was a J&W GC column HP-5MS [(5%-phenyl)-methyl-polysiloxane], 30 m length, 0.25 mm internal diameter and 0.25 µm film thickness.

ESI-MS. Mass spectra were recorded by using electrospray ionization (ESI) with a Bruker Esquire 3000 plus ion-trap mass spectrometer instrument equipped with an ESI Ion Trap LC/MSn system.

NMR. ¹H-NMR and ¹³C-NMR spectra were recorded on a Bruker 400 MHz instrument (100 MHz) at 298 K. For ¹H-NMR analysis, 5 mg of PyC were dissolved in 1.0 mL of CDCl₃. Chemical shifts were reported in ppm with the solvent residual peak as the internal standard (CDCl₃: δ _H = 7.26 ppm). For ¹³C-NMR analysis, 40 mg of PyC were dissolved in CDCl₃. Chemical shifts were reported in ppm with the solvent residual peak as the internal standard (CDCl₃: δ _H = 77.16 ppm). 2D ¹H-¹H COSY and ¹H-¹³C HSQC spectra were acquired with the same parameters used for 1D experiments. The number of scans was adjusted based on the sample concentration to ensure an adequate signal-to-noise ratio.

2.5.2. Characterization of poly(S-*co*-PyC) copolymers

Solubility. 100 mg of poly(S-*co*-PyC) copolymers were suspended in 10 mL of solvent and stirred at room temperature for 24 hours. After one hour at rest, the dispersions were visually inspected and were classified as “yes”, “partially”, and “no”, depending on whether the copolymer was soluble, partially soluble, and insoluble, respectively. The calculation of the Hansen solubility parameters for poly(S-*co*-PyC) was performed by applying the Hansen solubility sphere representation of miscibility, as already reported by some of the authors.⁵² The fitting sphere program was adapted and solved in the MATLAB environment using the Nelder–Mead simplex algorithm.⁵²

Elemental analysis. The characterization was performed by using a Costech ECS mod.4010 analyzer.

NMR. ¹H-NMR and ¹³C-NMR were performed as reported above for the pyrrole compounds.

FT-IR. The analyses were performed by using a Nicolet IS5 instrument. For the preparation of each sample, 10 mg of PyC or poly(S-*co*-PyC) materials were pulverized in 1.0 gram of KBr. The mixture was pressed by using a hydraulic press and the pill was then analyzed.

Thermal characterization. The DSC instrument was a Mettler Toledo 823e model, serial number 5128266639. 5 mg of the product were put in an alumina crucible.

A DSC thermal scan for the characterization of poly(S-*co*-PyC) was performed as follows: the sample was first heated from 25 °C to 155 °C, at a heating rate of 10 °C min⁻¹, to eliminate the thermal history of the material. Then, an isothermal ramp was applied at 155 °C for 5 minutes. The sample was cooled from 155 °C to -30 °C by following a dynamic cooling ramp of 20 °C min⁻¹. An isothermal ramp at -30 °C for 5 minutes was applied to stabilize the system. The sample was then heated from -30 °C to 155 °C at 20 °C min⁻¹. All the thermal cycles were performed under a nitrogen atmosphere, with a flow rate of 50 mL min⁻¹. The evaluation of the glass transition temperature (T_g) was performed taking into account the last thermal ramp. The T_g of each copolymer was determined by calculating the maximum point of the curve obtained from the first derivative of the second heating. Origin was used as the calculation program.

GPC. For the determination of the molecular weight of poly(S-*co*-PyC), a GPC-MALS system was described as follows: every sample was dissolved in THF with a concentration of 3.0 mg mL⁻¹. Then, the sample was filtered by using a PTFE filter having a diameter of 45 µm. Each analysis was then performed in a tetrahydrofuran (THF) mobile phase with a Waters 1515 isocratic pump running three 5 µm TSKgel columns (Tosoh,

pore size 300 × 7.8 mm) at a flow rate of 1 mL min⁻¹ at 30 °C. A triple detector Wyatt, having a Multi Angle Light Scattering MALS miniDAWN TREOS, a ViscoStar II viscosimeter and an Optilab T-rEX detector, was used. Molar masses were calculated using Empower software (Waters).

2.5.3. Characterization of elastomeric composites

Crosslinking. The crosslinking reaction of rubber composites was carried out at 170 °C for 20 minutes. 5 g of crude rubber compound were introduced in a rheometer, a rubber process analyser (RPA, Alpha Technologies, Hudson, OH, USA). First, a strain sweep was performed at low deformations (0.1%–25% strain), before the crosslinking step. Then the sample was kept at 50 °C for ten minutes and subjected to another strain sweep always at 50 °C. Subsequently, crosslinking at 170 °C for 20 minutes was performed, with an oscillation angle of 6.98% and a frequency of 1.7 Hz. The torque *versus* time curve, the minimum achievable torque (M_L), the maximum achievable torque (M_H), the time needed to have a torque equal to $M_L + 1$ (t_{S1}), and the time needed to reach 90% of the maximum torque (T_{90}) were measured.

Shear dynamic mechanical properties. On crosslinked samples, a first strain sweep (0.1–25% strain amplitude) was performed at 50 °C, and then the sample was kept in the instrument at the minimum strain amplitude (0.11) for 10 minutes to achieve fully equilibrated conditions. Finally, a strain sweep (0.1–25% strain amplitude) was performed with a frequency of 1 Hz. The measured properties were shear storage, shear loss and the ratio G''/G' (G' , G'' and $\tan \delta$).

3. Results and discussion

3.1. Synthesis of dipyrrole compounds (PyC)

HMDP and EDP were synthesized *via* the Paal–Knorr reaction,^{45,46} with 2,5-HD as the dicarbonyl compound and hexamethylenediamine or ethylenediamine as the primary amines, as shown in Fig. 2.

The reaction was carried out without using solvents and catalysts for two hours at room temperature (EDP) or by heating the binary mixture for three hours (HMDP). The reaction temperature was set at the lowest possible value to reduce the impact on the environment^{53,54} and to obtain a high yield, taking also into consideration the boiling point of the diamines (116 °C for ethylenediamine and 204 °C for hexamethylenediamine). Water was the only co-product and the dipyrrole compounds were washed with water and collected without any additional purification steps. The chemical purity of the pyrrole compounds was assessed by means of GC-mass, ESI-

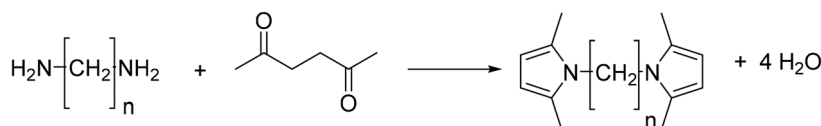


Fig. 2 Synthesis of EDP ($n = 2$) and HMDP ($n = 6$) *via* the Paal–Knorr reaction.



mass, and ^1H and ^{13}C -NMR analyses, and by-products were not detected. The yield was excellent and very good:^{55,56} 92% and 88% for HMDP and EDP, respectively. The results of the characterization are reported in the ESI:[†] the ^1H -NMR, ^{13}C -NMR, GC-mass and ESI-mass results of HMDP are shown in Fig. S.1–S.4.[†] The same characterization techniques were applied to EDP and the results are reported in Fig. S.5–S.8.[†] The atom efficiency was 73% and 65% for HMDP and EDP, respectively. HMDP and EDP were isolated and then used without any further purification.⁵¹

3.2. Synthesis of poly(S-*co*-PyC) copolymers

The poly(S-*co*-PyC) copolymers were synthesized as shown in the reaction scheme in Fig. 3.

The experimental conditions reported in the first work on inverse vulcanization¹¹ were adopted. Details are in the Experimental part. In brief, sulfur was kept at 185 °C for 10 minutes, obtaining a viscous red liquid. Then, either HMDP or EDP was added and the reaction mixture was stirred for 10 minutes at 185 °C. Various S/PyC weight ratios were used for the preparation of the copolymers, from 0.7 to 4, as reported in Table 1. When the weight ratio S/HMDP = 9 was used as the weight ratio, a copolymer was not obtained (data are in the ESI, from Fig. S.9–S.12†). Hence, the sulfur in the copolymers was from about 41 wt% to about 80 wt%, in line with the range reported in the literature on sulfur copolymers by inverse vulcanization.^{11–26} As reported in Table 1, the content of the pyrrole ring in the copolymers was from about 14 wt% to about 41 wt%. The nominal average length of the sulfur sequences (expressed as the number of sulfur atoms) between the pyrrole compounds was (about) from 3 to 17.

3.3. Characterization of poly(S-*co*-PyC) copolymers

3.3.1. Solubility. The solubility of the copolymers was checked in a series of solvents, using a Hildebrand solubility parameter⁵⁷ in the range from 3.9 to 30.1: hexane, toluene, dichloromethane, chloroform, tetrahydrofuran, acetone, dimethyl sulfoxide, and water. The Hansen⁵⁸ and Hildebrand parameters of all the solvents are reported in Table S.1 in the ESI† and the details of the solubility tests are in the Experimental part. The copolymers were completely soluble in chloroform and dichloromethane, while they were partially

soluble in toluene, acetone and dimethyl sulfoxide. Complete insolubility was observed in water and hexane. Experimental results are reported in Table S.2 in the ESI.†

The solubility tests were useful to assess the absence of residual comonomers (sulfur and HMDPP) in the copolymers. Indeed, sulfur and HMDPP are soluble in toluene. By extracting the sample of entry 1 with toluene, neither sulfur nor HMDP was detected in the extracted product.

Moreover, the results of the solubility tests were used to estimate the Hansen solubility parameters (HSPs) and the Hildebrand solubility parameters of the copolymers. It is worth commenting here that the Hansen method accounts for molecular interactions between a solvent and solute and allows for the estimation of solubility parameters based on three specific interactions: δ_D (dispersion), δ_P (polar), and δ_H (hydrogen bonding). The total δ_T (Hildebrand) solubility parameter can then be calculated as the sum of the squares of the HSPs. As commented above, all the copolymers revealed the same solubility behaviour (see Table S.2†). The evaluation of HSPs, δ_D , δ_P , δ_H , and δ_T was done for the copolymer from entry 1, following the procedure described in the Experimental section, by applying the algorithm already reported.⁵² The solubility sphere for the copolymer from entry 1, which encompasses the good solvents and excludes the bad ones, is to be seen in Fig. 4. The following values for the solubility parameters (MPa^{1/2}) were obtained: $\delta_D = 18.0$, $\delta_P = 7.7$, $\delta_H = 6.7$, and $\delta_T = 20.7$. These values are close to the values of the most common rubbers, whether saturated such as polyolefin elastomers (EPDM) or unsaturated such as NR, and are particularly close to the values of the polar poly(butadiene-*co*-acrylonitrile) rubber (NBR) (see Table S.3†). Hence, it can be reasonably hypothesized that the poly(S-*co*-PyC) copolymers are soluble in rubber matrices and can efficiently behave as crosslinking agents.

3.3.2. Elemental analysis. The analysis was performed on the poly(*S*-co-HMDP) samples of entry 1 and entry 3. The results are reported in Table 3.

The values of weight% for carbon, nitrogen and sulfur are very close to the theoretical ones (see Table 1), calculated on the basis of the monomers added to the polymerization flask. The samples were not purified and these results indicate that the comonomers were not lost during the polymerization. In light of the findings from the solubility tests and from the

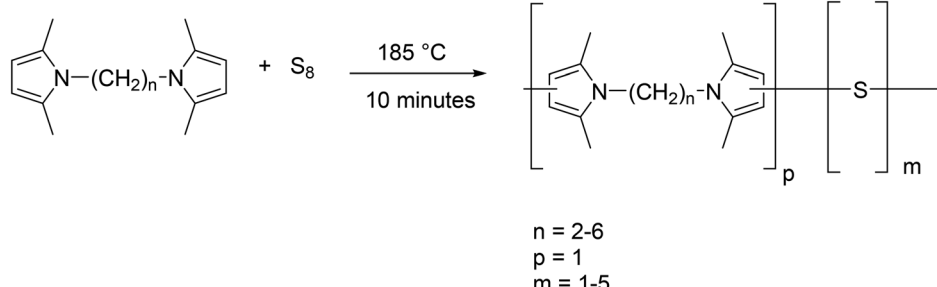


Fig. 3 Synthesis of poly(S-*co*-PyC) copolymers.

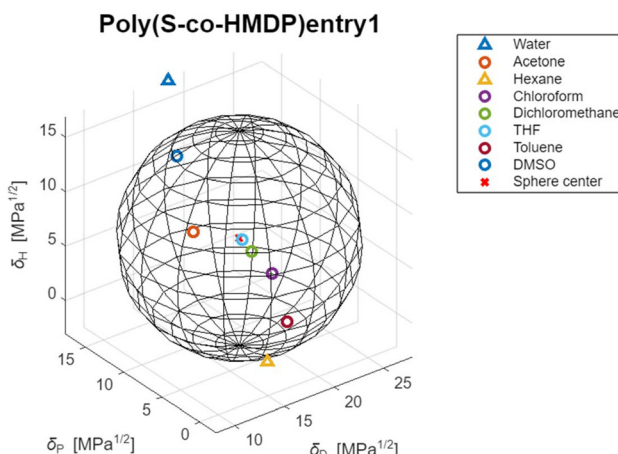


Fig. 4 Hansen solubility sphere of poly(S-co-HMDP) with 41% sulfur (entry 1 of Table 1).

DSC analysis (see below in the text), it can be commented that the amount of sulfur and PyC added to the reaction flask reflects the chemical composition of the copolymers.

3.3.3. Differential scanning calorimetry. In Fig. 5, the DSC traces of sulfur (Fig. 5A), HMDP (Fig. 5B) and the poly(S-PyC) copolymers (Fig. 5C) can be seen.

Elemental sulfur revealed endothermic peaks at about 108 °C and about 120 °C, due to the melting of orthorhombic and monoclinic phases. The melting temperature of HMDP was 108 °C.

The endothermic peaks of sulfur and the pyrrole compound could not be detected in the DSC traces of the poly(S-co-HMDP) copolymers from entry 1 to entry 5, with sulfur/HMDP weight ratios from 0.7 to 2.3, and in the DSC trace of the poly(S-co-EDMP) copolymer. The results from solubility tests, elemental analysis and DSC indicate that these copolymers were prepared without residual comonomers and by-products. The *E* factor⁵¹ was evaluated for these preparations, for the whole synthetic pathway, from diamine and sulfur to the copolymer, with reference to the organic compounds, neglecting the water co-product of the PyC's synthesis. Details are provided in Table S.4 in the ESI.† An almost null *E* factor was found. Indeed, the values were 0.11 for the poly(S-co-HMDP) copolymers and 0.07 for the poly(S-co-EDMP) copolymer.

The DSC trace of the copolymer from entry 6, prepared with 80% sulfur by weight, reveals the presence of an endothermic peak at about 110 °C, which could be due to both comonomers, the monoclinic form of sulfur and HMDP. The high

reactivity of PyC with sulfur, documented by some of the authors,⁴³ could support the first hypothesis. Indeed, the copolymer from entry 6 was washed with toluene, obtaining a yellow solution. The DSC analysis of the washed copolymer did not reveal any peak at 110 °C and the IR analysis of the extracted product did not reveal any trace of HMDP.

All the copolymers were found to be amorphous. The glass transition temperature was found to consistently increase with the content of the pyrrole compound. The poly(S-co-HMDP) copolymers, with a weight% of the pyrrole ring from 14% to 41%, showed a *T_g* from about -2 °C to about 38 °C.

In the literature on sulfur copolymers, it was documented that *T_g* increases with the amount of the organic comonomer. The highest values were reported for dicyclopentadiene¹⁹ and for 5-ethylidene-2-norbornene²¹ as the comonomers, 115 °C and 89 °C, respectively. In Fig. 5D, the dependence of *T_g* on the weight% of the pyrrole ring is shown. *T_g* tends to reach a plateau, which is achieved at a pyrrole ring weight content higher than 40%. The *T_g* value of the poly(S-co-EDP) copolymer reveals the effect of the spacer between the pyrrole rings: a smaller number of methylene groups led to a higher weight% of the pyrrole ring and hence to a higher *T_g*.

3.3.4. Gel permeation chromatography. GPC analysis of poly(S-co-HMDP) copolymers was carried out in THF as the solvent, as described in the Experimental part. The values of number average molecular weight *M_n*, weight average molecular weight *M_w* and dispersity (*D* = *M_w*/*M_n*) are reported in Table S.5 in the ESI.†

Copolymers were obtained in a range of *M_n* from 1.7×10^3 to 9.0×10^3 g mol $^{-1}$. The latter value is higher than those reported in the literature, for sulfur copolymers with α -limonene,¹⁴ dipentenes,²⁴ terpenes,¹⁹ 1,3-diisopropylbenzene,¹¹ and styrene.^{15,58} Only copolymers with a hyperbranched structure, such as those obtained with benzoxazine and cardanol, revealed higher values of molecular mass. The molecular mass values obtained for sulfur copolymers in the literature are collected in Table S.6 in the ESI.† These results could be explained by the longer spacer between the reactive groups (the pyrrole rings). A pretty narrow molecular weight distribution, from 1.2 to 1.7, was obtained.

3.3.5. Infrared analysis. The chemical nature of functional groups present in the copolymers was confirmed by FT-IR spectroscopy. In Fig. 6, the FT-IR spectra of HMDP and poly(S-co-HMDP) copolymers from entry 1 to entry 6 and entry 8 are reported.

In all the spectra reported in Fig. 6, there are easily detectable bands related to the stretching vibrations of -CH₂ and

Table 3 Elemental analysis of poly(S-co-HMDP) copolymers

Entry ^a	Carbon, wt%	Standard deviation	Hydrogen, wt%	Standard deviation	Nitrogen, wt%	Standard deviation	Sulfur, wt%	Standard deviation
1	40.0	±0.2	6.06	±0.3	4.96	±0.1	20.3	±0.5
3	49.8	±0.2	7.90	±0.3	6.05	±0.1	23.2	±0.5

^a See Table 1.

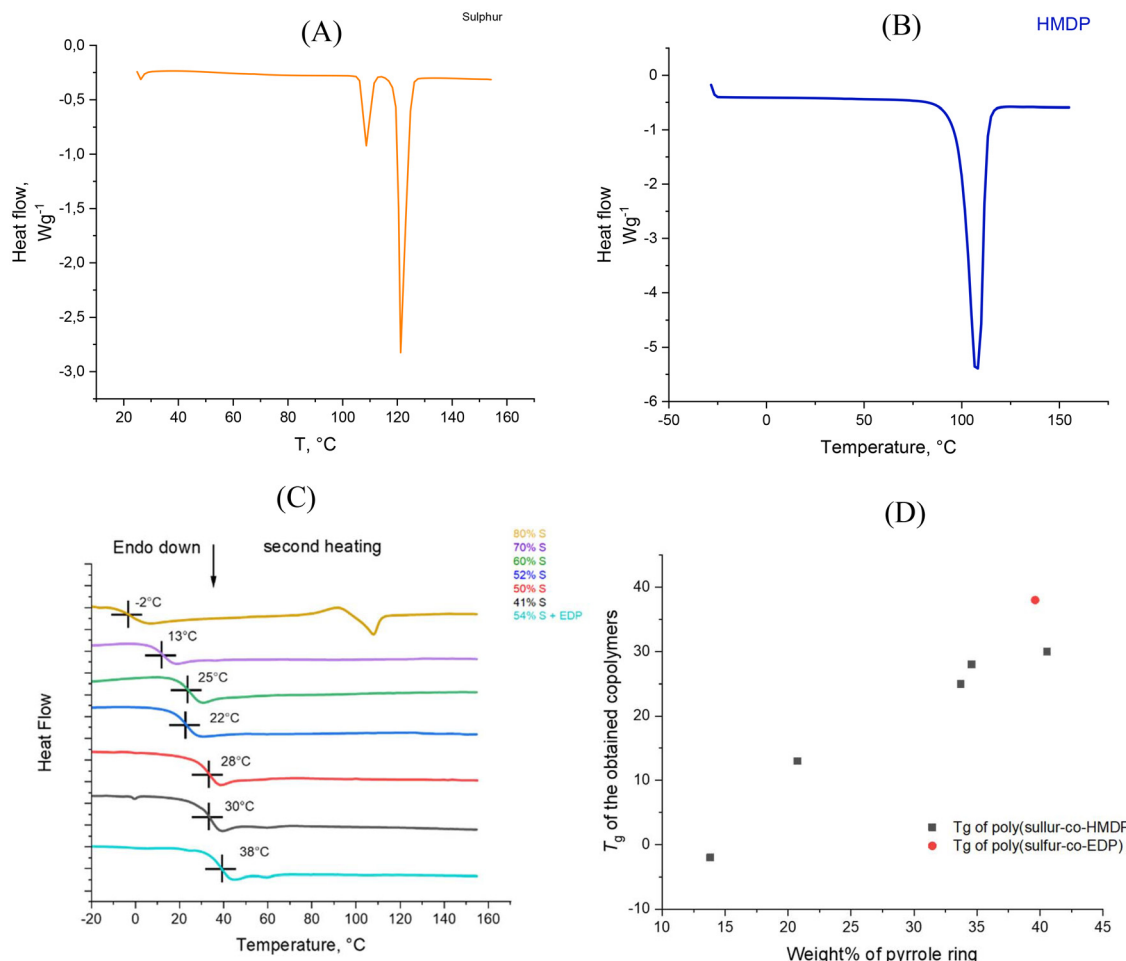


Fig. 5 DSC thermal analysis of (A) pristine sulfur, (B) pristine HMDP, (C) second heating of poly(S-co-PyC) materials, and (D) correlation between the molar percentage of pyrrole rings in the sulfur-based copolymer and T_g .

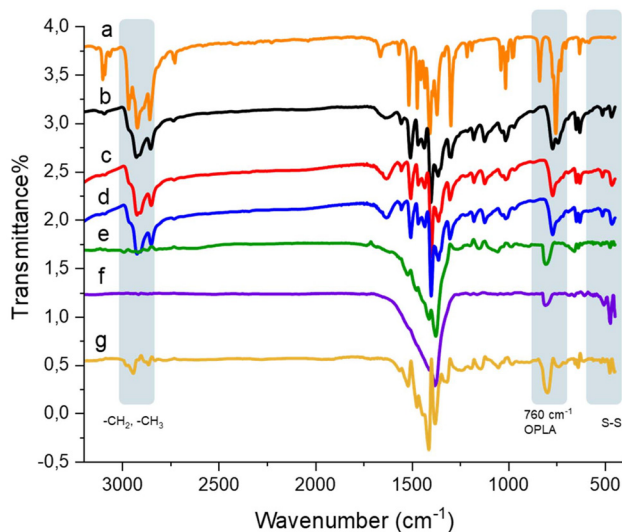


Fig. 6 FT-IR spectra of (a) pristine HMDP and poly(S-co-HMDP) materials with weight% of sulfur equal to (b) 41%, (c) 50%, (d) 52%, (e) 60%, (f) 70% and (g) 80%.

-CH₃ groups. In HMDP (Fig. 6a), these signals are in the typical region from 2700 to 3000 cm⁻¹. These bands are broader in the spectra of poly(S-co-HMDP) copolymers (Fig. 6b-f). This finding could be due to the substitution with sulfur of the methyl group in the benzylic position of the pyrrole ring. Another important IR fingerprint for pyrrole compounds is the signal at 760 cm⁻¹ and the out-of-plane (OPLA) signals related to C-H in the β position of the pyrrole rings.⁵⁹ Also in the FT-IR spectra reported in Fig. 6, the OPLA signals are detectable at 760 cm⁻¹. In the IR spectra of the poly(S-co-HMDP) copolymers, the OPLA signals are at higher wavenumber values; they are at 773 cm⁻¹ for the copolymers with a weight % of sulfur content ranging from 41% to 52% (Fig. 6b-d) and at 814 cm⁻¹ for the copolymers having a higher sulfur content, ranging from 60 to 80 wt% (Fig. 6d-f). These shifts could be explained by the substitution with sulfur, in the case of the carbon atom in the β position of the pyrrole ring. In the IR spectra of the poly(S-co-HMDP) copolymers, the peak at 516 cm⁻¹ is due to the -S-S- sequences,^{60,61} and it appears to increase with the amount of sulfur in the copolymer.



3.3.6. NMR analysis. The microstructure of the poly(S-*co*-HMDP) copolymer was studied by means of nuclear magnetic resonance (NMR) spectroscopy. ^1H - and ^{13}C -spectra were recorded for all the copolymers. The spectra can be seen in Fig. S.13–S.24 in the ESI.† 2D ^1H - ^1H -COSY and 2D ^1H - ^{13}C HSQC spectra were recorded for poly(S-*co*-HMDP) from entry 1 of Table 1. The NMR results for poly(S-*co*-HMDP) from entry 1 are discussed in the following text.

^1H -NMR analysis. In Fig. 7, the ^1H -NMR spectra of pristine HMDP and poly(S-*co*-HMDP) are shown.

For the attribution of the peaks, the ppm value of the hydrogen atom signal (7.26 ppm) was used as the reference. The assignment of the sharp singlets and the multiplets in the spectrum of HMDP is shown in Fig. 7A. The spectrum of poly(S-*co*-HMDP) appears indeed different: new peaks are present, there are multiplets instead of the sharp singlets of pristine HMDP and signals are broader.

By examining the aromatic part of the polymer spectrum between 5.5 and 6.7 ppm (the area of heterocyclic aromatics),

which gives indications of the pyrrole ring, two signals can be detected: a broad singlet at 5.8 ppm and a multiplet centered at 6.5 ppm. These signals can be attributed, respectively, to 3,4 protons in the β positions of the pyrrole ring without sulfur atoms and to 3',4' protons in the pyrrole ring substituted by sulfur atoms. The pyrrole ring without sulfur atoms should be considered a chain end, whereas the pyrrole ring with sulfur atoms propagates the chain, as shown in the chemical structure in Fig. 7B. By assuming that the substitution with sulfur occurred in position 3', the signal at lower fields can be attributed to 4'. If substitution with sulfur occurred in position 4', the signal at lower fields can be attributed to 3'.

Relevant changes can be observed, at high fields, for the signal due to the methyl groups on carbon atoms 2 and 5. The singlet at 2.21 ppm in the spectrum of HMDP has become a multiplet, whose peaks are in the range between 2.17 ppm and 2.21 ppm and a new group of peaks is between 2.32 ppm and 2.37 ppm. These signals can be attributed to both the methyl group on carbons 2 and 5 of the pyrrole ring not substituted

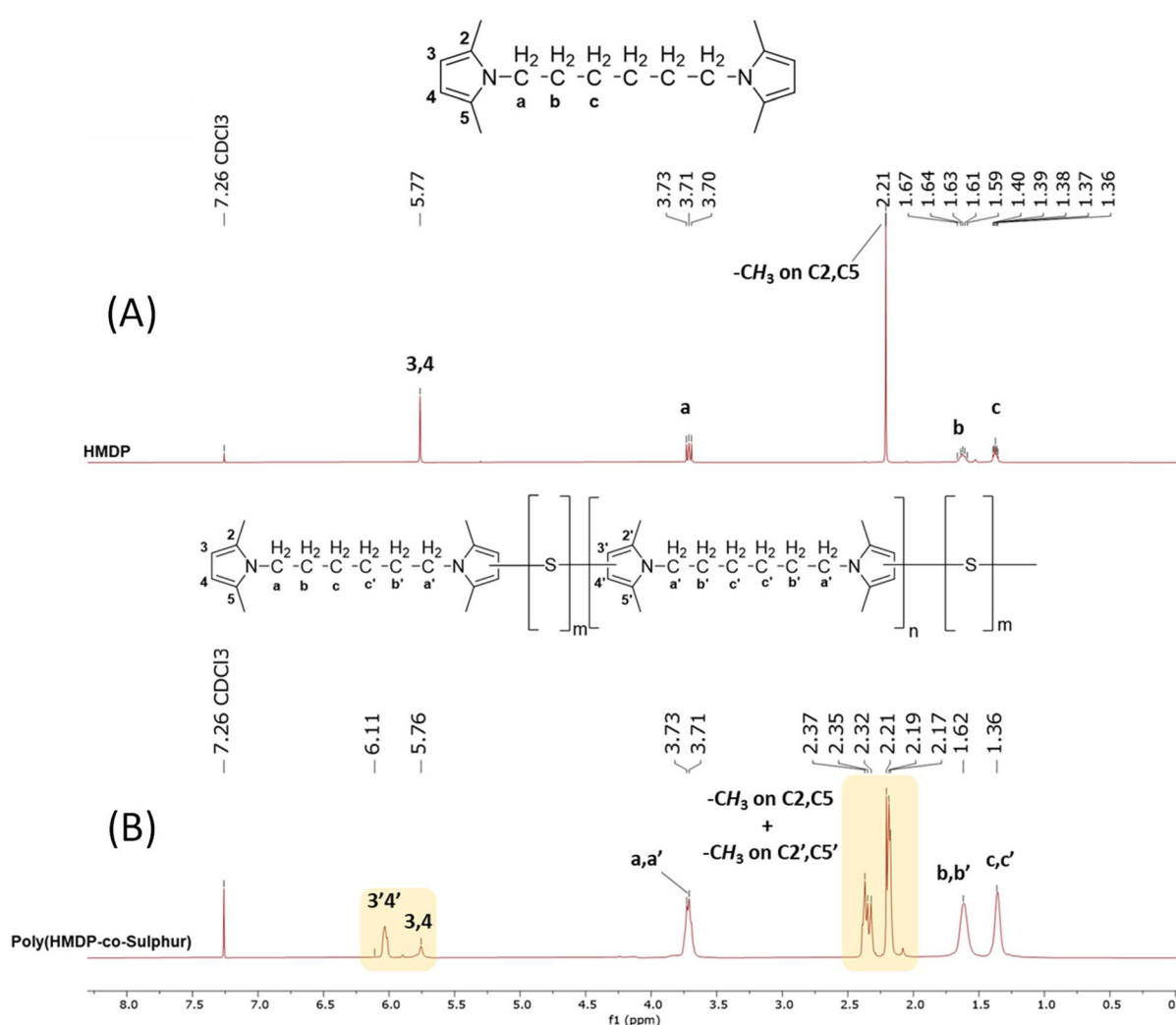


Fig. 7 ^1H -NMR spectra (CDCl_3 , 400 MHz) of: (A) pristine HMDP and (B) poly(S-*co*-HMDP) from entry 1 of Table 1.



by sulfur atoms (the chain end) and to the methyl group on the carbon atoms, either (2') or (5'), adjacent to a carbon atom in the β position carrying a sulfur atom, either (3') or (4'). By assuming that the substitution with sulfur occurred in position 3', the signal at higher fields can be attributed to the methyl group in position 5'.

The spectrum of poly(S-*co*-HMDP) does not provide indications of the presence of sulfur on the methyl groups on carbon atom 2 and carbon atom 5. Indeed, new signals are not present in the region between 3.8 and 4.2 ppm, which is characteristic of the methylene group close to the pyrrole ring.

The signals of all the methylene units between the two pyrroles are more complex but are centered at the same chemical shift as in the spectrum of HMDP. The complexity of the signals could be attributed to the overlap between the peaks due to the methylenes (a, b, and c) close to the pyrrole ring free of sulfur atoms (the chain end) and the peaks due to the methylenes (a', b', and c') close to the pyrrole ring bearing sulfur atoms (in the repeating unit).

On the basis of the available experimental findings, multiple substitutions by sulfur atoms of the same pyrrole ring, that would result in small shifts of the methyl signals, could not be excluded.

The assignments of the 1D ^1H -NMR spectrum were further investigated by performing a COSY experiment. The ^1H - ^1H COSY spectrum of poly(S-*co*-HMDP) is shown in Fig. 8.

In the COSY spectrum, it is possible to distinguish the correlations based on the protons of the CH_3 group belonging either to a pyrrole ring free of sulfur atoms or to a pyrrole ring bearing sulfur atom(s). The aromatic portion of the spectrum

shows the following correlations: 4'-(CH_3 on C5') and 3,4-(CH_3 on C2, C5). This is indeed a revealing finding, as it clarifies that under the multiplet between 2.17 and 2.31 ppm there are both the signals of CH_3 in the positions C2 and C5 of the pyrrole ring without sulfur and the signal of CH_3 in the position C5' of the pyrrole ring with sulfur atoms. This finding confirms the substitution with the sulfur atoms of the pyrrole ring.

A correlation emerges between the protons in position a,a' and the protons in position b,b' and hence between b,b' and c, c'. This confirms the previous statement: it is not possible to distinguish between the methylene groups belonging either to a repeating or to a terminal HMDP unit.

^{13}C -NMR analysis. The ^{13}C -NMR spectra of pristine HMDP and the poly(S-*co*-HMDP) copolymer from entry 1 of Table 1 are shown in Fig. 9.

The assignment of the peaks associated with HMDP is shown in Fig. 9A.

New signals were detected in the ^{13}C -NMR spectrum of poly(S-*co*-HMDP) (Fig. 9B).

The peaks at 109.99 ppm and 127.13 ppm are assigned to the C3 and C4 and to the C2 and C5 carbon atoms in the unsubstituted pyrrole ring, respectively.

The new signals due to the carbon atoms in the pyrrole ring substituted with sulfur are: C2' at 134.17 ppm, C5' at 127.13 ppm, C3' at 111.23 ppm, and C4' at 108.53 ppm. In the enlargement of the ^{13}C -NMR spectrum in Fig. 9C, new signals can be detected. They suggest the presence in the pyrrole ring of carbon atoms bearing two sulfur atoms (3" and 4"). This hypothesis could justify the lower intensity of the C4' signal.

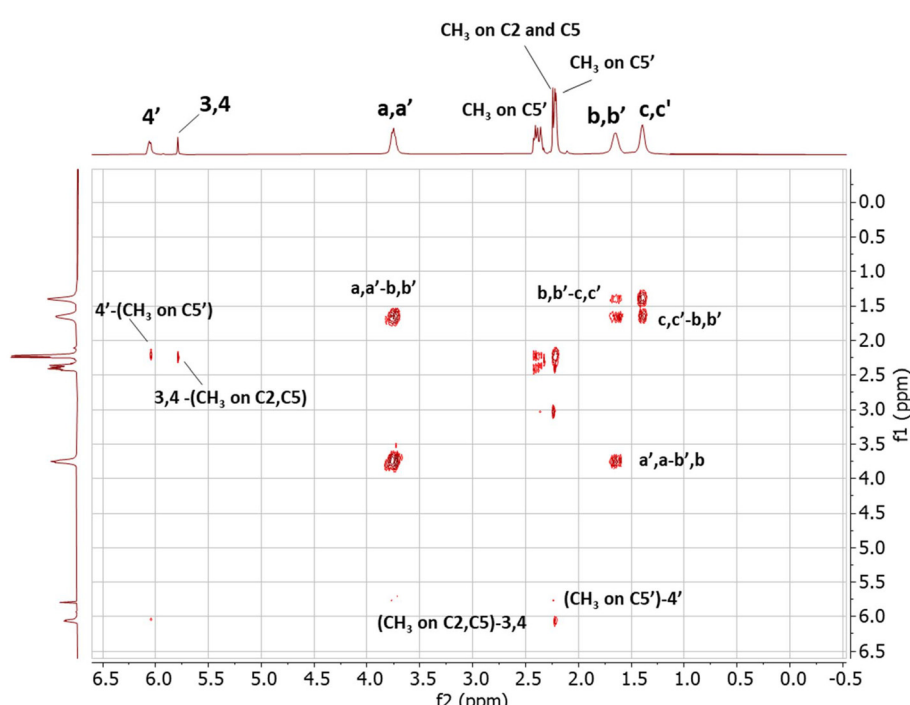


Fig. 8 ^1H - ^1H COSY spectrum of poly(S-*co*-HMDP) from entry 1 of Table 1 in CDCl_3 .



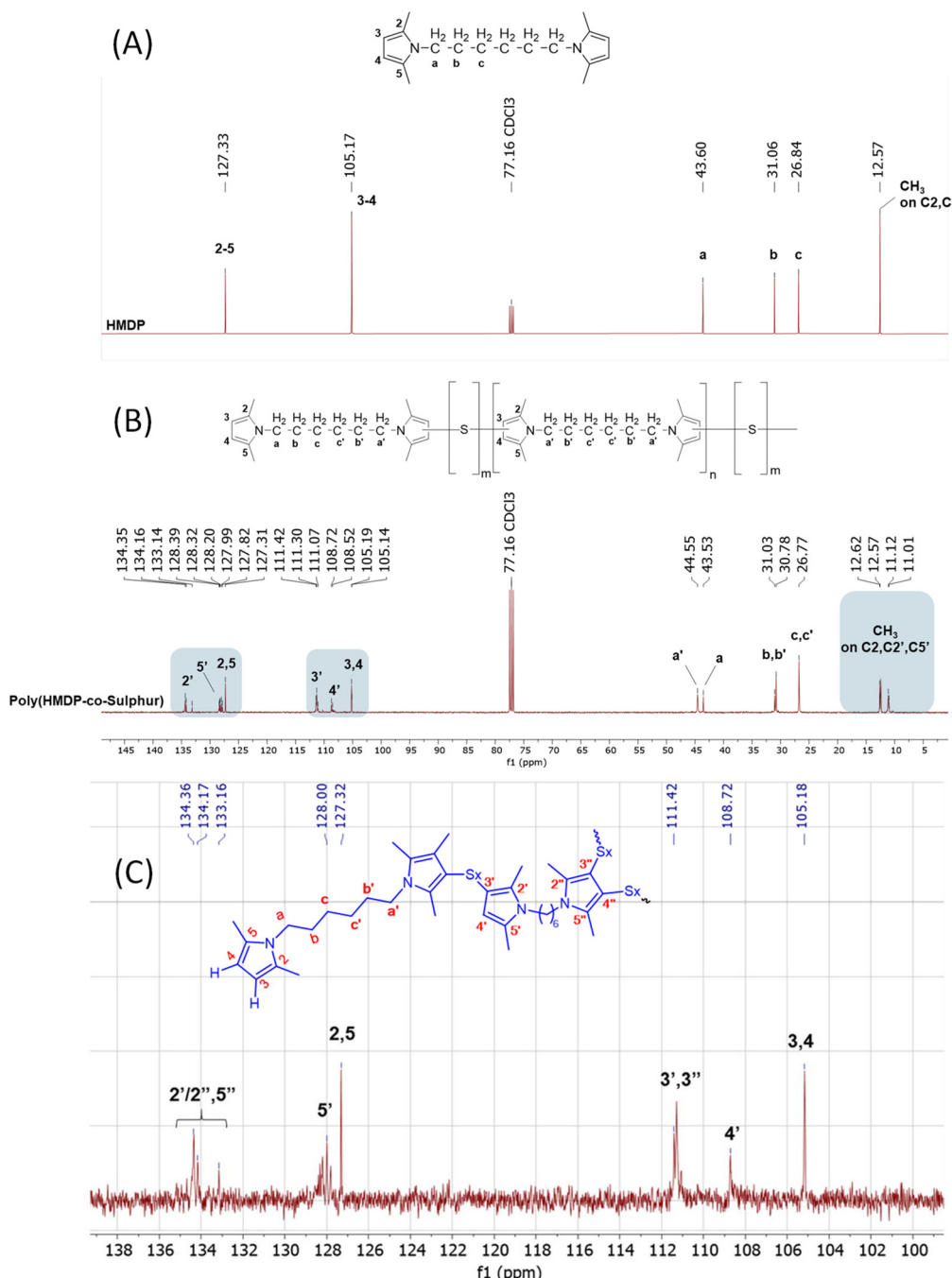


Fig. 9 ^{13}C -NMR spectra (CDCl_3 , 100 MHz) of (A) HMDP and (B) poly(S-co-HMDP) from entry 1 of Table 1. (C) ^{13}C -NMR spectrum in the region between 100 and 140 ppm.

The signals of $2''$ and $5''$ could fall in the region between 133 and 135 ppm.

New signals were also observed in the typical NMR region for aliphatic hydrocarbons, between 25 and 45 ppm and between 10 and 13 ppm. In particular, the signals of the methyl groups either in the unsubstituted pyrrole (C2 and C5) or in the substituted pyrroles (C2' and C5') are at 12.43, 12.24, and 10.82 ppm.

In contrast to what was observed in the ^1H NMR spectrum, a different chemical shift was observed for the CH_2 directly linked to the nitrogen atom, when the pyrrole was without sulfur atoms (Ca at 43.34 ppm) or was substituted with sulfur (C'a' at 44.36 ppm).

The correlation between ^1H -NMR and ^{13}C -NMR was performed by means of HSQC experiments. The ^1H - ^{13}C HSQC spectrum is shown in Fig. 10.

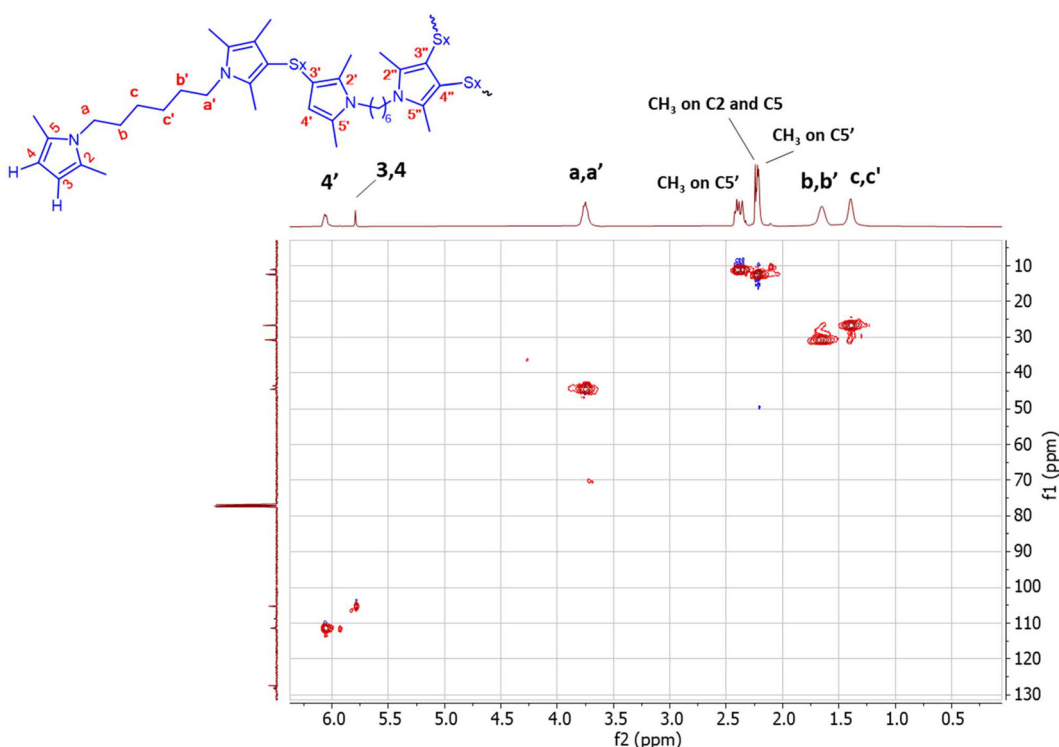


Fig. 10 ^1H - ^{13}C HSQC spectrum of poly(S-co-HMDP) from entry 1 of Table 1 in CDCl_3 .

In the HSQC spectrum, both the H-4 to C4 correlation and the $\text{H-4}'$ with $\text{C4}'$ correlation are observed. In addition, a correlation between $\text{H-a}'$ and $\text{C-a}'$ is revealed. It is possible to distinguish between the $\text{C-b}'$ and $\text{C-c}'$ methylenes because of their respective correlations with $\text{H-b}'$ and $\text{H-c}'$. These results confirm the structure proposed above.

The assignments reported in the text above appear to be confirmed by the spectra of the copolymers from the other entries, which are shown in the ESI.[†] In particular, the $^1\text{H-NMR}$ spectrum in Fig. S.17[†] of the poly(s-co-HMDP) copolymer, which has a higher sulphur content, reveals a higher intensity for the protons on $\text{C4}'$, to indicate a higher amount of pyrrole ring substituted with sulphur atoms. The $^{13}\text{C-NMR}$ spectrum of the same copolymer, shown in Fig. S.18 in the ESI,[†] reveals a lower intensity for the peak due to the carbon atom $\text{4}'$ and a higher intensity for the peaks attributed to carbon atoms $\text{3}'$ and $\text{3}''$, to suggest a substitution with sulphur of both the carbon atoms in the β positions of the pyrrole ring.

The $^1\text{H-NMR}$ and $^{13}\text{C-NMR}$ spectra of EDP and poly (S-co-EDP) are shown in Fig. S.25 and S.28,[†] respectively, and discussed in the ESI.[†]

3.3.7. The structure of the poly(s-co-HMDP) copolymers and the mechanism for their formation. The NMR findings indicate that the chain of poly(s-co-HMDP) propagates through the carbon atoms in the β position of the pyrrole ring. The mono-substitution of the pyrrole ring seems to be favored but, on the basis of the available results, a further substitution could not be excluded. There are no indications that the

methyl group in the alpha position of the ring participates in the chain propagation. Hence, it can be hypothesized that the polymer has, prevailingly, a linear structure.

As reported in the Introduction, this work was motivated by the radical reactivity of the pyrrole ring; however, it could be hypothesized that the pyrrole derivative could act as a weak base, due to the lone pair on the nitrogen atom, which is involved in resonance within the aromatic pyrrole ring. Such a weak base could induce the ionic polymerization of elemental sulfur. Two reaction pathways could be hypothesized. They are shown in Fig. S.29 in the ESI.[†] To examine this hypothesis, the actual reactivity of such a lone pair should be considered. The lone pair on the nitrogen, involved in the resonance in the pyrrole ring, should not be able to react with acids or, in general, with electrophiles. The protonated pyrrole has a $\text{p}K_a = 4$ and hence the starting base has a $\text{p}K_b = 10$.

Moreover, the ionic mechanism could hardly lead to the propagation of the chain. In fact, as shown in Fig. S.30 in the ESI,[†] the anionic sulfur chain end could likely abstract an hydrogen atom, thus restoring the aromaticity of the ring.

The radical pathway appears to be the preferred one.

3.4. Elastomer composites with the poly(S-co-HMDP) copolymer as the sole crosslinking agent

The most important application of unsaturated elastomers is in tyre tread compounds. Typically, styrene-butadiene rubber from solution anionic polymerization is used, optionally in combination with a minor amount of poly(1,4-cis-isoprene)



from *Hevea brasiliensis*. As anticipated in the Introduction, the crosslinking of the elastomer chains is performed with a sulfur based system containing primary accelerators such as sulphenamides and optionally secondary accelerators such as guanidines or serinol derivatives.⁶² There is a dramatic need for simpler crosslinking systems, to move in the direction of sustainability and to have better reproducibility. Ideally, the crosslinking ingredient should be based on only one ingredient. It is acknowledged that sulfur cannot be such an ingredient, as the crosslinking is very slow and the reversion is pronounced.⁸ In this work, as mentioned in the Introduction, the poly(S-*co*-HMDP) copolymer was used as the sole crosslinking agent for an elastomer composite suitable for tire tread compounds, with furnace carbon black as the reinforcing filler. The reactivity of the poly(S-*co*-HMDP) copolymer with the elastomer chains was supposed to be due to the cleavage of the

sulfur bonds, followed by either radical or ionic reactions with the polymer chains.

Two composites were prepared with the poly(S-*co*-HMDP) copolymer from entry 1. The copolymer contained 41 wt% sulfur and had 3 sulfur atoms as the average length of the sulfur sequence. The composites were prepared in the absence and in the presence of a bicyclic amidine base, such as 1,5-diazabicyclo(5.4.0)undec-7-ene, as a coagent. DBU was used to promote the ionic reactivity of sulfur with the unsaturated elastomers. The composite recipes are reported in Table 2.

3.4.1. Curing. The curing reaction of the composites was conducted at 170 °C for 20 minutes and monitored by performing a rheometric test, as described in the Experimental section. The increase in torque was taken as an indication of the vulcanization reaction. The dependence of the torque on the curing time is shown in Fig. 11 below. The values of minimum torque (M_L), maximum torque (M_H), induction vulcanization time (t_{s1}), optimum vulcanization time (t_{90}) and vulcanization rate are reported in Table S.7 in the ESI.†

The poly(S-*co*-HMDP) copolymer is an effective crosslinking agent for unsaturated elastomers, as shown by the low induction time and by the increase in torque with the vulcanization time. The addition of DBU does not affect the viscosity (M_L) of the composite, whereas it leads to a substantial increase in the maximum torque (M_H) (about 40%) and the curing rate. Hence, a beneficial effect on the crosslinking reaction was obtained by promoting the ionic reactivity of sulfur with the elastomer chains.

3.4.2. Dynamic-mechanical properties in shear mode. The dynamic-mechanical properties of the crosslinked samples were determined in shear mode using strain-sweep experiments, by applying a sinusoidal stress at a frequency of 1 Hz, with a strain amplitude range from 0.1% to 25%, at 50 °C, as described in more detail in the Experimental section. The storage modulus (G'), loss modulus (G''), and $\tan \delta$ (G''/G') were measured. The graphs showing the dependence of G' and the $\tan \delta$ on the strain amplitude are visible in Fig. 12a and b for the composites without and

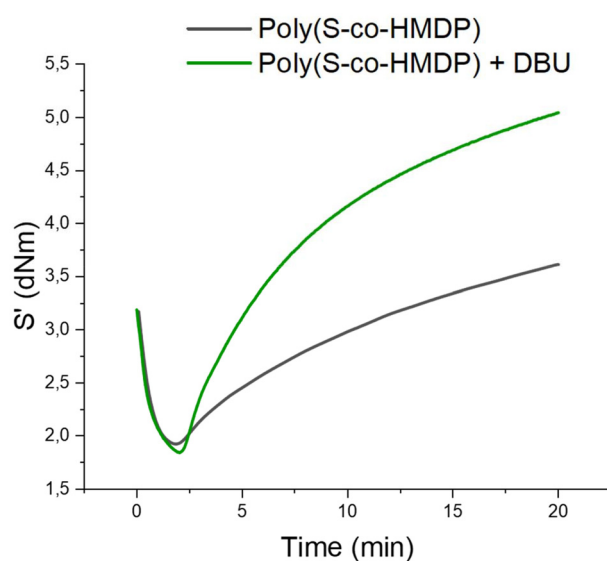


Fig. 11 Curing curves of elastomer composites in Table 2.

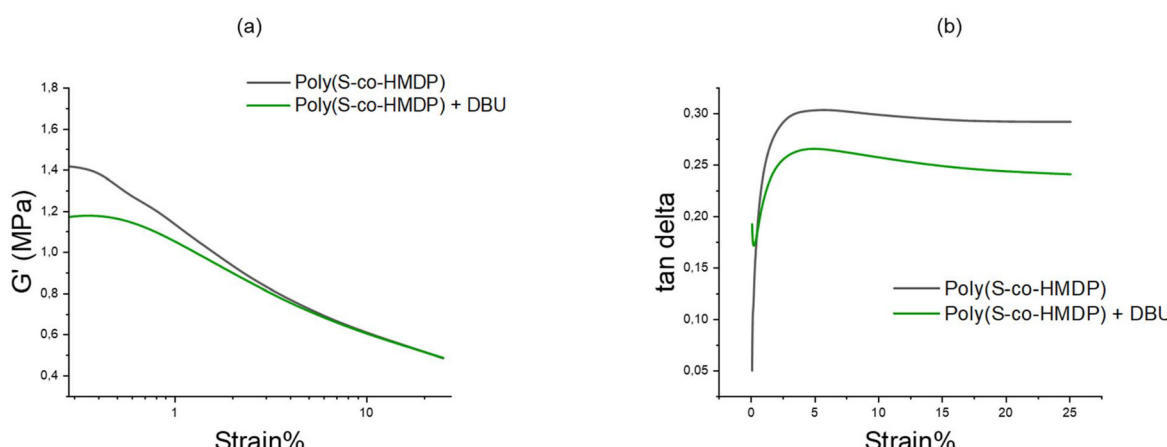


Fig. 12 (a) G' vs. strain% and (b) $\tan \delta$ vs. strain% of the elastomer composites in Table 2.



with DBU, respectively. Data obtained from the experiments are in Table S.8 in the ESI.†

Both composites revealed a reduction of the G' modulus with the strain amplitude, as expected, considering that the filler was above its percolation threshold. The non-linearity of the storage modulus, a phenomenon known as the Payne effect,^{63–66} results from the disruption of the filler network. The composites with DBU show lower Payne effects and lower Tan delta values. The lower Payne effect is due to a lower value of G' at minimum strain. Indeed, the G' value at maximum strain was the same for both composites and this leads to the assumption that there is no appreciable difference between the crosslinking networks. Hence, it could be hypothesized that with the copolymer/DBU system, a better dispersion of the filler is obtained. To account for these findings, a reaction of the vulcanization system with CB could be hypothesized. The grafting of sulfur copolymers with CB has been recently reported⁶⁷ and a lower Payne effect was observed in SBR based composites. An ionic mechanism for the reaction of sulfur with polycyclic aromatic compounds, such as carbon black, was hypothesized by some of the authors.²⁷ The results reported here are preliminary. They demonstrate that poly(S-*co*-HMDP) can act as a sole crosslinking agent. The traditional vulcanization system based on sulfur and one or more accelerators definitely leads to better properties. For example, for a composite based on SBR and CB as the reinforcing filler, the values of M_H and of G' at high strain are remarkably higher.⁶⁸ Hence, further research is needed.

4. Conclusions

Innovative sulfur copolymers were prepared using di-pyrrole compounds by exploiting the reactivity of pyrrole rings with thiyl radicals. Di-pyrrole compounds, HMDP and EDP, were obtained from the reaction of primary amines and a dicarbonyl compound: HMD, EMD and HD in the present study. The precursors of the PyCs could arise from biosources and from an EOL polymer, thus promoting circular materials. In this study, the synthesis of HMDP and EDP was characterized by excellent and very good yields, 92% and 88%, and by atom efficiencies of 73% and 65%, respectively, with water as the only co-product. Poly(S-*co*-PyC) copolymers were synthesized in a wide range of chemical compositions by applying the typical experimental conditions of inverse vulcanization, without observing any residual comonomers or by-products. Without considering the water used to wash the di-pyrrole compounds, the synthesis from the pristine precursors to the copolymers was characterized by an almost null E factor, down to 0.11 for HMDP and to 0.07 for EDP. Poly(S-*co*-PyC) copolymers were amorphous and were characterized by a wide range of T_g , from $-2\text{ }^\circ\text{C}$ to $38\text{ }^\circ\text{C}$, with higher values obtained with higher values of pyrrole contents. The pyrrole rings allow us to achieve higher values of T_g compared to those of sulfur copolymers reported in the literature. A poly(S-*co*-HMDP) copolymer, with 41 wt% sulfur content, was then used as an innovative cross-

linking agent for elastomer composites based on SBR. The sulfur copolymer with the di-pyrrole compound plays a twofold role in the elastomer composite: as a crosslinking agent of the elastomer chains and as a grafting agent of carbon black. This allows us to achieve lower hysteresis and hence lower dissipation of energy. These results are preliminary. Further research should be focused on enhancing the reactivity of the copolymers with elastomer chains and modulating the structure of the crosslinking network. It would be definitely interesting to use poly(S-*co*-PyC) copolymers in combination with the traditional ingredients of vulcanization. However, these innovative copolymers pave the way for a new generation of more sustainable elastomer composites.

Data availability

Data are contained within the article and its ESI.†

Conflicts of interest

The authors declare no competing financial interest.

Acknowledgements

The authors wish to thank Pirelli Tyre for the financial support of the research and for financing the PhD of Simone Naddeo.

References

- 1 R. L. Rudnick and S. Gao, Composition of the Continental Crust, in *Treatise on Geochemistry*, ed. R. L. Rudnick, Executive Editors: H. D. Holland and K. K. Turekian, Elsevier, 2003, vol. 3, pp. 1–64, 659 pp. ISBN 0-08-043751-6.
- 2 F. H. Peckham, The Medical Properties of Sulfur, *Boston Med. Surg. J.*, 1849, **41**(2), 41–44.
- 3 M. Mitchard, Sulfur compounds used in medicine, *Drug Metab. Drug Interact.*, 1988, **6**(3–4), 183–202.
- 4 M. E. Rodriguez, The role of spices and minerals in Greek ritual, *Classicum*, 2012, **38**(1), 8–14.
- 5 H. E. Brown, Rubber and plastics, *Sch. Sci. Math.*, 1947, **47**(3), 264–266.
- 6 W. H. Davies and W. A. Sexton, Chemical constitution and insecticidal action. 1. Organic sulfur compounds, *Biochem. J.*, 1948, **43**(3), 461.
- 7 H. Morawetz, History of rubber research, *Rubber Chem. Technol.*, 2000, **73**(3), 405–426.
- 8 A. Y. Coran, Vulcanization, in *The science and technology of rubber*, ed. J. E. Mark, B. Erman and M. Roland, Academic press, 2013, ch. 7.
- 9 M. J. Worthington, R. L. Kucera and J. M. Chalker, Green chemistry and polymers made from sulfur, *Green Chem.*, 2017, **19**(12), 2748–2761.



10 J. A. Ober, Materials Flow of Sulfur, Open-File Report 02-298. 2003, U.S. Department of the Interior, U.S. Geological Survey. <https://pubs.usgs.gov/of/2002/of02-298/> accessed 27 December 2016.

11 W. J. Chung, J. J. Griebel, E. T. Kim, H. Yoon, A. G. Simmonds, H. J. Ji and J. Pyun, The use of elemental sulfur as an alternative feedstock for polymeric materials, *Nat. Chem.*, 2013, **5**(6), 518–524.

12 Z. Sun, M. Xiao, S. Wang, D. Han, S. Song, G. Chen and Y. Meng, Sulfur-rich polymeric materials with semi-interpenetrating network structure as a novel lithium–sulfur cathode, *J. Mater. Chem. A*, 2014, **2**(24), 9280–9286.

13 M. Arslan, B. Kiskan, E. C. Cengiz, R. Demir-Cakan and Y. Yagci, Inverse vulcanization of bismaleimide and divinylbenzene by elemental sulfur for lithium sulfur batteries, *Eur. Polym. J.*, 2016, **80**, 70–77.

14 M. P. Crockett, A. M. Evans, M. J. Worthington, I. S. Albuquerque, A. D. Slattery, C. T. Gibson and J. M. Chalker, Sulfur-Limonene Polysulfide: a material synthesized entirely from industrial by-products and its use in removing toxic metals from water and soil, *Angew. Chem., Int. Ed.*, 2016, **55**(5), 1714–1718.

15 Y. Zhang, J. J. Griebel, P. T. Dirlam, N. A. Nguyen, R. S. Glass, M. E. Mackay and J. Pyun, Inverse vulcanization of elemental sulfur and styrene for polymeric cathodes in Li–S batteries, *J. Polym. Sci., Part A: Polym. Chem.*, 2017, **55**(1), 107–116.

16 T. Thiounn, M. K. Lauer, M. S. Bedford, R. C. Smith and A. G. Tennyson, Thermally-healable network solids of sulfur-crosslinked poly (4-allyloxystyrene), *RSC Adv.*, 2018, **8**(68), 39074–39082.

17 S. Z. Khawaja, S. V. Kumar, K. K. Jena and S. M. Alhassan, Flexible sulfur film from inverse vulcanization technique, *Mater. Lett.*, 2017, **203**, 58–61.

18 S. Akay, B. Kayan, D. Kalderis, M. Arslan, Y. Yagci and B. Kiskan, Poly (benzoxazine–co–sulfur): An efficient sorbent for mercury removal from aqueous solution, *J. Appl. Polym. Sci.*, 2017, **134**(38), 45306.

19 D. J. Parker, H. A. Jones, S. Petcher, L. Cervini, J. M. Griffin, R. Akhtar and T. Hasell, Low cost and renewable sulfur-polymers by inverse vulcanisation, and their potential for mercury capture, *J. Mater. Chem. A*, 2017, **5**(23), 11682–11692.

20 S. Shukla, A. Ghosh, U. K. Sen, P. K. Roy, S. Mitra and B. Lochab, Cardanol benzoxazine–Sulfur Copolymers for Li–S batteries: Symbiosis of Sustainability and Performance, *ChemistrySelect*, 2016, **1**(3), 594–600.

21 J. A. Smith, X. Wu, N. G. Berry and T. Hasell, High sulfur content polymers: The effect of crosslinker structure on inverse vulcanization, *J. Polym. Sci., Part A: Polym. Chem.*, 2018, **56**(16), 1777–1781.

22 N. A. Lundquist, M. J. Worthington, N. Adamson, C. T. Gibson, M. R. Johnston, A. V. Ellis and J. M. Chalker, Polysulfides made from re-purposed waste are sustainable materials for removing iron from water, *RSC Adv.*, 2018, **8**(3), 1232–1236.

23 T. Tian, R. Hu and B. Z. Tang, Room temperature one-step conversion from elemental sulfur to functional polythioureas through catalyst-free multicomponent polymerizations, *J. Am. Chem. Soc.*, 2018, **140**(19), 6156–6163.

24 S. Silvano, I. Tritto, S. Losio and L. Boggioni, Sulfur-dipentene polysulfides: from industrial waste to sustainable, low-cost materials, *Polym. Chem.*, 2022, **13**(19), 2782–2790.

25 S. Zhang, L. Pan, L. Xia, Y. Sun and X. Liu, Dynamic polysulfide shape memory networks derived from elemental sulfur and their dual thermo-/photo-induced solid-state plasticity, *React. Funct. Polym.*, 2017, **121**, 8–14.

26 I. Gomez, A. F. De Anastro, O. Leonet, J. A. Blazquez, H. J. Grande, J. Pyun and D. Mecerreyes, Sulfur polymers meet poly (ionic liquid) s: bringing new properties to both polymer families, *Macromol. Rapid Commun.*, 2018, **39**(21), 1800529.

27 S. Musto, V. Barbera, V. Cipolletti, A. Citterio and M. Galimberti, Master curves for the sulfur assisted cross-linking reaction of natural rubber in the presence of nano- and nano-structured sp^2 carbon allotropes, *EXPRESS Polym. Lett.*, 2017, **11**(6), 435–448.

28 R. A. Jones and G. P. Bean, *The Chemistry of Pyrroles: Organic Chemistry: A Series of Monographs*, Academic Press, 2013, vol. 34.

29 A. Fürstner, Chemistry and biology of roseophilin and the prodigiosin alkaloids: a survey of the last 2500 years., *Angew. Chem., Int. Ed.*, 2003, **42**(31), 3582–3603.

30 G. L. Petri, V. Spano, R. Spatola, R. Holl, M. V. Raimondi, P. Barraja and A. Montalbano, Bioactive pyrrole-based compounds with target selectivity, *Eur. J. Med. Chem.*, 2020, **208**, 112783.

31 E. Mateev, M. Georgieva and A. Zlatkov, Pyrrole as an important scaffold of anticancer drugs: recent advances, *J. Pharm. Pharm. Sci.*, 2022, **25**, 24–40.

32 S. Guerra, V. Barbera, A. Vitale, R. Bongiovanni, A. Serafini, L. Conzatti and M. Galimberti, Edge functionalized graphene layers for (ultra) high exfoliation in carbon papers and aerogels in the presence of chitosan, *Materials*, 2019, **13**(1), 39.

33 G. Marino, Quantitative aspect of electrophilic substitution in furan, thiophene, pyrrole, and other five-membered heteroaromatic systems, *Chem. Heterocycl. Compd.*, 1973, **9**(5), 537–545.

34 B. Jolicoeur, E. E. Chapman, A. Thompson and W. D. Lubell, Pyrrole protection, *Tetrahedron*, 2006, **62**(50), 11531–11563.

35 I. A. Jacobson Jr, H. H. Heady and G. U. Dinneen, Thermal reactions of organic nitrogen compounds. I. 1-Methylpyrrole, *J. Phys. Chem.*, 1958, **62**(12), 1563–1565.

36 J. M. Patterson, J. Brasch and P. Drenchko, Synthesis and pyrolysis of some cycloalkano [a] pyrroles, *J. Org. Chem.*, 1962, **27**(5), 1652–1659.

37 I. A. Jacobson Jr and H. B. Jensen, Thermal reactions of organic nitrogen compounds. II. 1-n-butylpyrrole, *J. Phys. Chem.*, 1962, **66**(7), 1245–1247.

38 J. B. Conant and B. F. Chow, *J. Am. Chem. Soc.*, 1933, **66**, 3475.



39 R. J. Gritter and R. J. Chriss, Free-radical reactions of pyrroles, *J. Org. Chem.*, 1964, **29**(5), 1163–1167.

40 A. Priyadarshan, G. Tripathi, N. M. Venneti, K. Kishor, A. K. Singh and A. Kumar, Transition-Metal Free Arylation of Therapeutically Important Heterocycles, *ChemistrySelect*, 2024, **9**(19), e202400363.

41 A. K. Sahoo, A. Rakshit, A. Dahiya, A. Pan and B. K. Patel, Visible-light-mediated synthesis of thio-functionalized pyrroles, *Org. Lett.*, 2022, **24**(10), 1918–1923.

42 F. Denes, M. Pichowicz, G. Povie and P. Renaud, Thiyl radicals in organic synthesis, *Chem. Rev.*, 2014, **114**(5), 2587–2693.

43 D. Locatelli, A. Bernardi, L. R. Rubino, S. Gallo, A. Vitale, R. Bongiovanni and M. Galimberti, Biosourced Janus Molecules as Silica Coupling Agents in Elastomer Composites for Tires with Lower Environmental Impact, *ACS Sustainable Chem. Eng.*, 2023, **11**(7), 2713–2726.

44 U. Česárek, D. Pahovník and E. Žagar, Chemical recycling of aliphatic polyamides by microwave-assisted hydrolysis for efficient monomer recovery, *ACS Sustainable Chem. Eng.*, 2020, **8**(43), 16274.

45 C. Paal, Synthese von thiophen-und pyrrolderivaten, *Ber. Dtsch. Chem. Ges.*, 1885, **18**(2), 2251–2254.

46 L. Knorr, Einwirkung des Diacetbernsäureesters auf Ammoniak und primäre Aminbasen, *Ber. Dtsch. Chem. Ges.*, 1885, **18**(1), 299–311.

47 S. Naddeo, D. Gentile, F. Margani, G. Prioglio, F. Magaletti, M. Galimberti and V. Barbera, Pyrrole Compounds from the Two-Step One-Pot Conversion of 2, 5-Dimethylfuran for Elastomer Composites with Low Dissipation of Energy, *Molecules*, 2024, **29**(4), 861.

48 D. Hosler, S. L. Burkett and M. J. Tarkanian, Prehistoric polymers: rubber processing in ancient Mesoamerica, *Science*, 1999, **284**(5422), 1988–1991.

49 A. S. Aprem, K. Joseph and S. Thomas, Recent developments in crosslinking of elastomers, *Rubber Chem. Technol.*, 2005, **78**(3), 458–488.

50 Safety data sheet of 2-Mercaptobenzothiazole, Merk, <https://www.sigmadlrich.com/SE/en/product/aldrich/m3302>.

51 R. A. Sheldon, The E factor 25 years on: the rise of green chemistry and sustainability, *Green Chem.*, 2017, **19**(1), 18–43.

52 D. Locatelli, V. Barbera, L. Brambilla, C. Castiglioni, A. Sironi and M. Galimberti, Tuning the solubility parameters of carbon nanotubes by means of their adducts with Janus pyrrole compounds, *Nanomaterials*, 2020, **10**(6), 1176.

53 S. Madeddu, F. Ueckerdt, M. Pehl, J. Peterseim, M. Lord, K. A. Kumar, C. Krüger and G. Luderer, The CO₂ reduction potential for the European industry via direct electrification of heat supply (power-to-heat), *Environ. Res. Lett.*, 2020, **15**(12), 124004.

54 G. P. Thiel and A. K. Stark, To decarbonize industry, we must decarbonize heat, *Joule*, 2021, **5**(3), 531–550.

55 A. I. Vogel and A. R. Tatchell, in *Vogel's Textbook of Practical Organic Chemistry*, ed. B. S. Furnis, A. J. Hannaford and P. W. G. Smith, Prentice Hall, 5th edn, 1996. ISBN 978-0-582-46236-6. Retrieved June 25, 2020.

56 R. H. Petrucci, W. S. Harwood and F. G. Herring, *General chemistry: principles and modern applications*, Prentice Hall, Upper Saddle River, NJ, 8th edn, 2002, p. 125. ISBN 978-0-13-014329-7. LCCN 2001032331. OCLC 46872308.

57 J. H. Hildebrand and R. L. Scott, *The Solubility of Nonelectrolytes*, Dover Publications, New York, NY, USA, 3rd edn, 1964.

58 C. M. Hansen, *Hansen Solubility Parameters: A User's Handbook*, CRC Press, Boca Raton, FL, USA, 2nd edn, 2007.

59 V. Barbera, L. Brambilla, A. Milani, A. Palazzolo, C. Castiglioni, A. Vitale and M. Galimberti, Domino reaction for the sustainable functionalization of few-layer graphene, *Nanomaterials*, 2018, **9**(1), 44.

60 D. Wang, Z. Tang, Z. Wang, L. Zhang and B. Guo, A bio-based, robust and recyclable thermoset polyester elastomer by using an inverse vulcanised polysulfide as a crosslinker, *Polym. Chem.*, 2022, **13**(4), 485–491.

61 M. Lee, Y. Oh, J. Yu, S. G. Jang, H. Yeo, J. J. Park and N. H. You, Long-wave infrared transparent sulfur polymers enabled by symmetric thiol cross-linker, *Nat. Commun.*, 2023, **14**(1), 2866.

62 V. Barbera, G. Leonardi, A. M. Valerio, L. Rubino, S. Sun, A. Famulari, M. Galimberti, A. Citterio and R. Sebastiani, Environmentally Friendly and Regioselective One-Pot Synthesis of Imines and Oxazolidines Serinol Derivatives and Their Use for Rubber Cross-Linking, *ACS Sustainable Chem. Eng.*, 2020, **8**(25), 9356–9366.

63 J. H. Dillon, I. B. Prettyman and G. L. Hall, Hysteretic and elastic properties of rubberlike materials under dynamic shear stresses, *J. Appl. Phys.*, 1944, **15**(4), 309–323.

64 W. P. Fletcher and A. N. Gent, Nonlinearity in the dynamic properties of vulcanized rubber compounds, *Rubber Chem. Technol.*, 1954, **27**(1), 209–222.

65 A. R. Payne, The dynamic properties of carbon black-loaded natural rubber vulcanizates. Part I, *J. Appl. Polym. Sci.*, 1962, **6**(19), 57–63.

66 N. Warasitthinon, A. C. Genix, M. Sztucki, J. Oberdisse and C. G. Robertson, The Payne effect: Primarily polymer-related or filler-related phenomenon?, *Rubber Chem. Technol.*, 2019, **92**(4), 599–611.

67 D. Wang, Z. Tang, S. Fang, S. Wu, H. Zeng, A. Wang and B. Guo, The use of inverse vulcanised polysulfide as an intelligent interfacial modifier in rubber/carbon black composites, *Carbon*, 2021, **184**, 409–417.

68 F. Magaletti, M. Galbusera, D. Gentile, U. Giese, V. Barbera and M. Galimberti, Carbon Black Functionalized with Serinol Pyrrole to Replace Silica in Elastomeric Composites, *Polymers*, 2024, **16**(9), 1214.

